Introduction to the movement of non-spherical bodies in flows of moderate or low number of Reynolds

Ing. Florentin R[1-2] 2, Ranalli G[2]., Dra. Miralles M [1-2-3]

[1]Universidad de Buenos Aires, Argentina, Fac. de Ingeniería, [2] Pontificia Universidad Católica Argentina, Argentina, Fac. De Ingeniería y Ciencias Agrarias, Argentina, rfloren@fi.uba.ar, monica_miralles@uca.edu.ar, [3]Universidad de Buenos Aires, Fac. de Arquitectura Diseño y Urbanismo, Argentina, guido.ranalli05@gmail.com

Abstract– This work describes a project designed for teaching ccontents related to fluid mechanic to engineering students and advanced students (academic internships) of the industrial design career of the Faculty of Architecture and Urbanism of the University of Buenos Aires (FADU- UBA). The project approach is to adhere to constructivist theories postulates, the guidelines of the TPACK group and the principles of project didactics (achieve an integrative, personalized, experiential, synthesizing, systematizing, conducive to the design process, participatory and selective teaching). It is considered strategic for the 21st century engineering education to train students in creative thinking and also on how to think about the new, about what is possible or what can be, enhancing their creativity in interdisciplinary work groups through academic activities that allow them to enhance their capacities thanks to the scientific knowledge acquired and the use of available technological tools.

A simple Stokes device (design and instrumentation) is presented and a series of experiments in the range of 0.2< Re < 10, which allow active learning of core concepts of fluid mechanics such as: deviation from sphericity of Stokes' law, the consequences of working with non-infinite flows, the sensitivity of the drag force to different flow patterns -particularly when the role of viscosity becomes predominant as the Re number is reduced-, the importance of the shape, the size, the relative orientation of the object to the flow direction, the surface treatment of the objects (whether natural or artificial), the mechanisms to reduce the drag force.

Keywords. —Education, Fluid Mechanics, Stokes' law, Reynolds number, deviation sphericity.

I. INTRODUCTION

In this work, oriented to the teaching of fluid mechanics in the degree, we resume a well-known experience for spheres based on Stokes' law. In laminar flows with low Reynolds number (Re<1) the viscous forces arising from the shearing motions of the fluid predominate over the inertial forces associated with the acceleration or deceleration of the fluid particles. They are called Stokes flows and Oseen regimes [1]. The distinguishing feature is the linearity or quasi-linearity of the underlying equations of motion.

The proposal presented in this paper comprises 2 parts. The first is the design and instrumentation of the equipment and the pieces to be used in the different experiments, presented in section II: Materials & Methods. And the experiments with spheres and non-spherical objects.

Next, we present the theoretical foundation of the proposed experiments. The reference of the equations used throughout this paper are presented in table I.

When a spherical particle of diameter "d" falls into a viscous flow, it is subjected to the action of the weight force (P), the thrust (E) and the viscous force (F_v). The initial movement is accelerated, and since F_v depends on velocity, it increases until it compensates for the net force (P-E). From then on, the velocity is constant and is called limit or terminal velocity (v_L). The number of Re is calculated according to equation (1) of Table I, where $V=v_L$ and "L"is a characteristic length. In the case of spheres L =d.

TABLE I
THEORETICAL EQUATIONS

$Re = \dfrac{\rho VL}{\mu}$	(1)	$v_L = \dfrac{g'}{k}$	(11)
$\mu = \dfrac{2r^2 g(\rho_E - \rho)}{9\,v_L}$	(2)	$t_L = \dfrac{2(\ln 0.005)\rho_E r^2}{9\mu}$	(12)
$v_L = v_m \left(1 + 2.4\dfrac{r}{R}\right)$ (Re<1)	(3)	$\alpha = \dfrac{x}{g't^2}$	(13)
$F_v = 3\pi\mu dv$	(4)	$\propto = \dfrac{1}{z} + \dfrac{1}{z^2}(exp\,(-z) - 1)$	(14)
$D = \dfrac{1}{2}\,C_D\,\rho\,A\,V^2$	(5)	$a = A\,m^{1/3}$, siendo $A = (3/4\pi\,\rho)^{1/3}$	(15)
$C_D = 24/Re\ (Re \cong 1)$	(6)	$a_s = \left(\dfrac{9\mu v}{2(\rho s - \rho)g}\right)^{1/3}$	(16)
$C_D = \dfrac{24}{Re} + \dfrac{6}{1+Re^{1/2}} + 0,4$ (Re >1)	(7)	$\dfrac{y}{l} > \dfrac{20}{Re}$	(17)
$\dfrac{dv}{dt} = \left(1 - \dfrac{\rho}{\rho_E}\right)g - \left(\dfrac{9\mu}{2\rho_E r^2}\right) = g'$ $- kv$	(8)	$V = \dfrac{4}{3}\pi a\,b^2$ a>b	(18)
$v(t) = \dfrac{g'}{k}(1-exp\,(-kt))$	(9)	$S = \dfrac{2\pi b\left[arctg\frac{\sqrt{a^2-b^2}}{b} + b\sqrt{a^2-b^2}\right]}{\sqrt{a^2-b^2}}$ a>b	(19/)
$x(t) = \dfrac{g'}{k} + \dfrac{g'}{k^2}(exp\,(-kt)\,-1)$	(10)		

A. Experiments with spheres

1) Viscosity measurement using smooth spheres of different diameters and materials (Stokes' law)

The viscosity can be found from (2) knowing the density of the sphere (ρ_E) and the radius (r), after measuring the velocity of the fall of the sphere (v_L). Depending on the number of Re, the v_L is calculated from the measured velocity (v_m), or

alternatively at Re<1, by applying the correction provided by Shoda [2] (see (3)), for finite flow (sphere falling in a tube of radius R).

The drag force (F_v) can be found by Stokes' law, equation (4), or by the general drag equation (5), taking into account two observations: the calculation of the C_D from equations (6) or (7), as appropriate, where the area (A) is the projected area (Re>1), or alternatively, the wetted area (Re<1), depending on whether the pressure or skin component predominates in the drag force, respectively [3].

2) Wall Effects

A series of spheres of increasing radius were used. The drag force was measured in each case, as was done in the previous experience. Since, in this case, the Reynold number interval is greater than 1, the C_D is calculated from equation (7), given by F.M. White [5], which is valid to up to $2x10^5$. The drag force is given in equation (5), where the characteristic length is the diameter of the sphere, and the area (A) is the projected one. The influence of the walls becomes more critical (drag increases) as the Re decreases and the skin component of drag force predominates.

3) Determination of the limit velocity from the equation of motion

Starting from the differential equation of movement (8), with the initial condition that at t = 0s, the v_o= 0m/s, the speed is obtained as a function of time (v(t)) (9). Its integration allows us to find the expression for the position of the object as a function of time (x(t)) (10). The limit speed will be the one that corresponds to long times (see (11)). The time in which it reaches the speed v_L can be predicted based on the criteria that $v(t)/v_L = 0.995$, measuring the temperature of the glycerin and taking the theoretical value of glycerin for the given temperature (12). Equation (10) can be dimensionless, giving rise to equation (14), from which the parameter ($\propto$) (13) can be obtained (considering (11)) and dividing both sides of the equation by $g't^2$). The parameter z is defined in equation (15). Then, measuring the position of the object and the time t>t_L, the experimental value of ($\propto$) is obtained (13). From finding the solution of the transcendental equation (14), the parameter z allows us to predict the value v_L and compare it with the experimental speed. Again, as in the previous case, the viscosity of glycerin can be determined from equation (2) and compared with the theoretical value taken from the monogram at the temperature of measurement [4]. Again, F_v or D can be found from equations (4) and (5).

B) Deviation from sphericity
1) The river pearls

In this experience, the goal was to study the deviation to Stokes' law as the object (river pearls) moves away from sphericity. In order to do so, the main criteria were to compare the so-called apparent radius (a_p) (see 15)) [6], obtained from the measurement of the mass and volume by immersion of the

spheroid, with the radius deduced from the law of Stokes, or Stokes radius (a_S), (see (16)), where ρ_S is the density of the spheroid.

2) Drag in textured spheres or with patterns of protruding shapes

In this case, the effect of surface patterns on the drag force is studied, and, when they have rough or non smooth surface.

3) The limit velocity in solids of revolution

Spheroidal pieces were designed by assembling halves of different solids of revolution to obtain symmetrical or asymmetrical prolate pieces. They were tested falling from both sides and measuring the limit speed in each case. A control sphere placed in its center allows comparison of the results. From this data and from the exposed surface, semi-empirical formulas can be found.

II. Material & Methods

A. The Stokes equipment
1) System Overview

Figure 1a) shows a schematic of the system designed for this work, Fig.1b) is a photograph of the finished kit, without fluid. It shows the transparent acrylic tube, 2.10 m high, 0.15 m outside diameter and 3mm wall thickness (internal diameter 0.147 m).

The tube is closed on the lower exterior with an acrylic lid and the upper part is open to the atmosphere. A ruler (attached to the length of the acrylic tube) allows you to measure the position of objects during the fall. A rectangular base with a frame of 0.78m x 0.50m (commercial steel profiles with a square section) ensures the stability of the system. To facilitate its movement, the base has 4 polyamide wheels welded under 4 wings, on the outside of the base frame (Fig.1c)). The structure has a prop consisting of a rectangular tube braced with two diagonal pieces to the base. A tilting bar serves as a support for the acrylic tube. Three clamps, attached to their respective crosspieces welded to the bar, allow for the tube to be fixed. The barrel features a sloped bottom bracket that transmits the weight of the tube and alleviates over-tightening of the clamps. A central pivot, which articulates in the hub of the prop, allows the inclination of the tube, keeping the base supported. By doing so, it allows the system to be transported through doors of different heights and facilitates its cleaning. All metal parts were treated with antirust coatings and painted with several layers of industrial synthetic enamel. To retrieve the samples without having to drain the tube, a simple lifting system was designed. It consists of a basket that can be moved along the tube by means of two nylon threads. The basket has holes in the lower part (Fig.1d)) to allow fluid to circulate during its movement. Two pulleys located at the upper end of the tube allow winding or unwinding the thread thanks to a crank (Fig. 1e)). A side drain tap (Fig.1 f)) allows the tube to be tilted and emptied into a suitable container. The system has a plug

centered on the bottom cover of the tube, which allows faster emptying (tube cleaning).

The viscous fluid used in this proposal was glycerin (100 %) since it allows the comparison of results with other authors. Since viscosity is a function of temperature, a Luft alcohol thermometer, ($\pm$ 1°C) is attached to the tube. A second mobile Luft thermometer, ($\pm$ 0.1°C). allows to study if there is a temperature gradient along the tube. Other viscous fluids can be used considering the corrosion of the acrylic to them. Once the tube is full, the verticality is checked with a level or plumb bob.
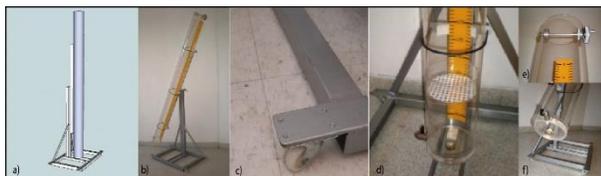

Fig. 1. Designed system a) system diagram b) photograph of the system, c) detail of the wheels of the base; d) sample collection basket; e) pulley system, f) bottom cover with side drain tap and drain plug.

2) Fall time measurements

A simple module was designed to measure the fall time of the object along the tube and to be able to calculate its terminal velocity inside the glycerin. It was designed considering circular sensing areas parallel to the tube section.

The minimum measurement module consists of three identical supports electronically instrumented, with the possibility of changing the distance between them.
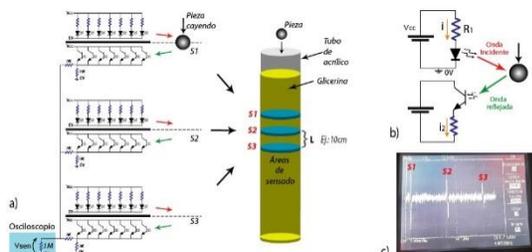

Fig. 2 Fall time measurement: a) measurement module, b) emitter and receiver subcircuit, c) signal interruption events.

The circuit of each support is divided into emitter and receiver, separated by a dividing wall. The emitter corresponds to the parallel of 10 identical circuits, each one formed by an infrared light-emitting photodiode, in series with a resistor R_1. Similarly, the receiver is formed by paralleling 10 identical circuits, each one formed by a phototransistor, sensitive to infrared light from the emitting photodiode, in series with a resistor R_2. (Fig. 2 a)).

The passage of the object is measured from the reflection of the light emitted by the photodiode on the object (Fig. 2b). As a result, the sum of the voltage across resistors R_2 is passed to a memory circuit, or to an oscilloscope with digital memory. Fig. 2.c) shows the signal from which time is determined on a Tektronix TDS 1012 oscilloscope (AC input coupling). The events marked as S1, S2 and S3 in the Fig. 3c) correspond to the instant in which the passage of the object interrupts the infrared beam. For the circuits, an IR 383 photodiode, a PT334-6C phototransistor, and R_1=220Ω, R_2=10 kΩ were used. The displayed signal was filtered with a 20 MHz low pass filter.

The time of each of the "S" events is determined for each experience, from defining a reference origin in the oscilloscope signal and selecting the appropriate time base (ms/div). In all cases the precision (0.2 div) is in the order of milliseconds.

The terminal speed of the object (v_L) is calculated as the arithmetic average of the 3 average speeds (each average speed measured from the ratio between the distance that separates two supports and the respective time interval), after verifying that the movement is rectilinear and uniform.

For the design of the supports, two basic spatial configurations were analyzed and tested: one annular and the other tangential to the tube. The tangential configuration turned out to be the most favorable because it presented the best coverage of the cross-sectional area of the tube (detection of objects of different sizes, dropped along the tube at different distances from the tube wall).

After several experimental tests with the tangential section, varying the number of emitters, it was fixed at 10. Fig. 3 a) shows the tangential support used with capacity for 10 receivers and emitters. In Fig. 3 b) shows the design of the coupling clamp.
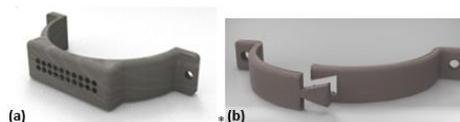

Fig. 3. Support of the module to measure the time of fall: a) tangential support; b) coupling clamp.

3) Design of parts and accessories

In the case of using the equipment without the lifting system, among the accessories designed, it has a top cover to prevent contamination of the fluid and various centering tubes (Fig. 4a)). The tubes are cylindrical in shape with a support base that fits over the top cover. The internal diameters range from 5mm to 50mm, in steps of 5mm. These tubes allow to ensure that the object falls along the axis of the cylinder and to minimize the asymmetries in the drag force due to the inevitable effect of the walls of the acrylic tube, even in symmetrical objects. Fig. 4b) shows -top view- designed accessories in the case of using the equipment with lifting system for retrieve samples.

Fig. 4. Design of parts and accessories a) Centering tubes, b) Top view of the centering system for the pieces adapted to the sample lifting system.

1) Design of solids of revolution

To study deviation from sphericity, we considered natural objects (river pearls) (Fig. 5 a)). and artificial objects. In the latter case, the pieces were made from half-shells with the same maximum cross-sectional diameter. This design allows the objects (test pieces) to be assembled in pairs, with the possibility of introducing a control sphere into the hollow core to normalize the results of the different experiments (Fig. 5b)).

The designs were thought with the double possibility of exchanging the halves to generate symmetrical or asymmetrical bodies. In this way, open a double possibility of studying the behavior of the flow on the object, depending on whether the front side faces the flow (direct flow or reverse flow) during the fall.

It also allows to study the v_L when the longitudinal axis of the objects is parallel or perpendicular to the flow direction [6].

The design of the pieces also contemplated smooth or textured spheres (Fig. 5c)); solids of revolution, (see Table VI), as well as "miscellaneous" shapes to study sphericity deviation. An example of these bodies is shown in Fig. 5d).
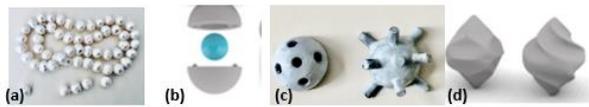

Fig. 5. Shapes to study sphericity deviation: a) river pearls, b) design principle for the pieces; c) textured spheres, d) miscellaneous shapes

III. Results

The results of the experiences detailed in section I.A) and I.B) are presented.

The number of measurements in each case is limited since it only aims to illustrate the didactic possibilities of the equipment designed for teaching fluid mechanics. The experiments require little time, and students can make a sufficient number of measurements during classes to integrate knowledge of statistical models known as the Student's t-test (t-test, $\alpha > 0.05$).

Mass was measured with a pocket scale (0-200 g) (±0.01 g). The geometric dimensions of objects with a Measy gauge (± 0.1 mm). The volume of the objects was measured by immersion in graduated cylinders (±0.1ml or 0.5 ml). The density of glycerin was the supplier's data sheet: QUIMIPUR, S.L.U (relative density ρ= 1.26 kg/m^3).

The polished spheres were made of glass or steel. For the rest of the pieces, 3D printing was used (PLA filament density, ρ_{PLA} =1.24 x 10^{3}g/m^3). In all cases the plans were made according to standard ISO-E

The spheres were chosen in a light color or were painted to increase the reflective power of infrared light and thus be better detected by phototransistors.

The speed of the fall and the measurement of time were carried out as detailed in section II.

The value of the acceleration of gravity in the Autonomous City of Buenos Aires was approximate to g = 9.80 m/s^2 according to [7]. The absolute errors were propagated according to the general error propagation formula for a physical quantity that is a continuous and derivable function of other measured physical quantities with their corresponding absolute error (see equation A5-16) in [8].

A. Experiments with smooth spheres
1) Determination of viscosity with smooth spheres of different sizes

For this experiment, the measurement module was placed below the middle of the tube and with the supports spaced at 0.5m from each other. The glycerin temperature was (23.0 ± 1°C). Table II presents the results of the determination of the glycerin viscosity and the drag force with spheres of increasing diameter of different materials.

The density of the glass measured from spheres 1, 3, and 5 match with the expected values for this material (2.5x10^3 kg/m^3), as well as sphere no. 3 made of steel (7.8 to 8.03 x10^3 kg/m^3). The density of sphere 4 is lower than that of steel due to heterogeneity (steel and plastic). In all cases, Re >1, so $v_L=v_m$ was considered.

In Table II ρ_E was calculated from the volume calculation (less error than the direct measurement of displaced volume, in ml), the number of Re considering: V = v_L, L = d (see (1)).

TABLE II
EXPERIMENTS WITH SMOOTH SPHERES

.	m (kg) 10^{-3}	d (m) 10^{-3}	vol$_T$ (m^3) 10^{-6}	vol$_E$ (m^3) 10^{-6}	ρ_{ST} kg/m^3 10^3	v_L (m/s)	μ (kg/ms)	Re	C$_D$	Fv (N) 10^{-1}	D (N) 10^{-1}
1	1.99	11.5	0.8	0.8	2.5	0.08	1.1	1.1	24.2	0.1	0.1
2	5.02	15.7	2.0	2.0	2.5	0.14	1.2	2.4	12.7	0.2	0.3
3	21.8	17.4	2.7	2.5	7.9	0.64	1.7	8.2	4.8	1.8	3.2
4	31.8	22.0	5.5	5.0	5.7	0.59	1.9	8.2	4.8	2.4	4.0
5	20.2	25.2	8.3	7.0	2.4	0.27	1.5	5,8	6.3	0.9	1.4

This experiment allowed us to:

a) Obtain the viscosity of glycerin at 23 ± 1°C. The value of μ = 1.3 ± 0.1 kg/ms was found from the arithmetic mean of the viscosities measured for the three glass spheres. This value coincides with that reported [4].

b) Verify that v_L increases with the diameter squared and refresh knowledge about graphing data with their errors. Obviously, viscosity can be found from the slope of the line v_L vs. d$_2$.

c) Highlight the sensitivity of the flow pattern around the spheres reflected in the increase of the Reynolds number in spheres 3 and 4. For Re < 10, the absence of any vortices is expected (creeping flow), but from Re close to 10, the onset of wake constriction is expected with the appearance of attached vortices.

d) Analyze the robustness of the Reynolds number in slow viscous flows, compared to that of this dimensionless parameter for turbulent flow.

2) Wall effects

The calculation of the drag force (equations (4) to (7)) is presented in the last columns of Table II. The drag force Fv emphasizes the predominance of viscous forces, while D considers the balance of both components (skin and pressure), always present. For Re≅1, both forces coincide (glass spheres), but as the Reynolds number slightly increases, the inertial forces become evident (steel spheres).

3) Prediction of the terminal velocity from the differential equation of motion

The objective of this experiment is to derive results from the differential equation of motion, so students can predict the time (t_L) at which the object reaches the terminal velocity (v_L). Then, for times $t>t_L$, the value of the parameter α can be found and the transcendental equation in the variable z can be solved using a simple computer program built by the students (or provided by the teachers), to predict v_L and compare it with the experimental value.

To do this, the measuring module is simply moved up the tube until the first support coincides with the level of glycerin in the tube (initial condition). The remaining supports are placed in known positions. The sphere is dropped, and the time of fall is measured as described in II.A.2).

To illustrate this experiment, sphere $n^o.2$ from experiment III.A.1 was used. The measured coordinates were x = 0.110 ± 0.001m at t = 0.250± 0.001s, the dimensionless parameter resulted in α = 0.362, z = 1.06 and the predicted terminal velocity (v_L*) is $v_L* = (1.4 ± 0.3)$ m/s.

B. Deviation from sphericity

1) The river pearls
River pearls were chosen for this experiment due to their bright white color (easy detection by sensors), small size, variety of non-spherical shapes, and low cost. Table III presents the results for 3 river pearls: "a_p" is the apparent radius (see (15)); "as" the Stokes radius (see (16)). Since in this case (Re<1), according to the inequality (3) provided by S. Voigt [9], the effect of the walls cannot be ignored, v_L must be calculated from v_m (see (3)).

It is observed that the parameters associated with river pearls do not show significant variations. The difference between the a_p radius (that of a sphere of the same volume as the pearl) and the Stokes radius (a_S) deduced from the Stokes law is significant. That is, a_S, in some way, reveals the influence of the flow pattern and is an order of magnitude larger than the geometric radius of the equivalent sphere (a_P).

If the river pearl is modeled as a sphere, the drag force can be calculated (assuming the viscosity has already been calculated) as was done in experiment II.A.1. In this case, C_D can be taken as 64/Re. The values obtained are coincident with those presented in Figure 5.4 (p.72) of reference [9] for spheres. Fv was calculated with $d = 2a_p$, and if D is calculated as a sphere with radius a_p, the values differ by an order of magnitude.

2) Drag in textured spheres or with patterns of protruding shapes.
A series of spheres with different surface textures were designed to evaluate the effect of introducing surface roughness in the v_L. All were materialized by 3D printing. For demonstration purposes, two designs are presented. The piece $n^o.1$ is a sphere with d= (21.4 ±1.0) mm formed by 2 halves with 5 circulars hollow holes on both sides (see Fig. 5c)). The second (no. 2) is a sphere of the same diameter, with the same pattern, but, in the place of the holes, there are 5 protruding cylinders orthogonal to the surface of the sphere of (7.1±1.0) mm and diameter (8.0±1.0) mm. In both cases the sphere $n^o.2$ from experiment III.1.A was placed in its center.

TABLE III
THE RIVER PEARLS

No.	m (kg) 10^{-3}	d_{max} (m) 10^{-3}	d_{min} (m) 10^{-3}	vol (m³) 10^{-6}	ρ kg/m³ 10^3	v_m (m/s) 10^{-1}	v_L (m/s) 10^{-1}	Re	a_p (m) 10^{-3}	as (m) 10^{-3}	C_D	Fv (N) 10^{-3}	D (N) 10^{-3}
1	0.85	9.1	8.5	3.5	2.4	0.6	0.6	0.5	4.0	30.0	47.84	3.3	13.0
2	0.90	9.2	8.6	3.7	2.4	0.6	0.6	0.5	4.0	16.3	89.82	3.0	12.0
3	0.83		7.6	3.2	2.6	0.6	0.6	0.2	4.0	15.4	94.74	3.0	12.0

TABLE IV
EXPERIMENTAL DATA FOR SPHERE WITH THROUGH-HOLE SURFACE PATTERN

m (kg) 10^{-3}	d (m) 10^{-3}	vol (m³) 10^{-6}	$ρ_S$ kg/m³ 10^3	v_L (m/s) 10
6.11	21.2	5.0	1.22	0.27

Table V presents the experimental data for object n°. 1. It is observed that after the glycerin enters the sphere, the vL is three times slower than that of the glass sphere at its core. This type of study allows for a deeper understanding of aspects related to the sensitivity of drag force to surface patterns and morphologies of objects. This is a topic of biological interest related to the control of drag in living organisms [9].

3) The speed limit in solids of revolution
For the study of non-spherical objects, the half-shells presented in Table V were designed. Three symmetrical objects (ellipsoid, paraboloid, and cone) and 4 asymmetrical objects were constructed from different combinations of the half-shells.

The theoretical model for these objects was that of a prolate ellipsoid with axes a > b. The major semi-axis "a" was determined from the maximum diameter of the object (d_{max}=2a), and the minor semi-axis "b" from the maximum width of the object's cross-section (d_{min}=2b). The theoretical volume and surface area exposed to the flow can be calculated using equations (18) and (19) or from the data on the surface and volume of the half-shells provided by the design software (see Table V).
Using these half shells, solids can be constructed that may be symmetrical (S-S, E2-E2, P3-P3, C-C) or asymmetrical (S-P, S-P2, P1-E1). The half-shells were glued with instant glue and the tightness of the piece was checked. Identical spheres to sphere no.4 in experiment III.A.1 were introduced into the hollow core

of each solid. Table VI shows the experimental data for E2 and sphere S-S (see Fig. VI photographs of S-S and E2).

TABLE V
HALF SHELLS OF DESIGNED SOLIDS OF REVOLUTION

Hemi-shells	m (kg) 10^{-3}	d_{min} (m) 10^{-3}	H (m) 10^{-3}	S (m^2) 10^{-4}	V (m^3) 10^{-6}
Sphere (S)	5	27.00	13.50	11.45	5.15
Paraboloid 1 (P1)	4	27.00	16.30	11.03	4.66
Paraboloid 2 (P2)	5	27.00	22.70	14.28	6.52
Paraboloid 3 (P3)	6	27.00	29.20	17.67	8.37
Ellipsoid 1 (E1)	7	27.00	21.60	16.23	8.22
Ellipsoid 2 (E2)	10	27.00	31.16	22.13	11.84
Cone (C)	4	27.00	27.38	12.95	5.22

TABLE VI
EXPERIMENTAL DATA E2 AND S-S SOLIDS

	m (kg) 10^{-3}	d_{min} (m) 10^{-3}	d_{max} (m) 10^{-3}	vol (m^3) 10^{-6}	ρ kg/m^3 10^3	v_L (m/s) 10^{-1}
E2	43.66	27,1	61,8	10.0	4.36	0.19
SS	36.12	26.8	26.3	9.8	3.68	0.47

When comparing the data of E2 with a) sphere n°.4, it can be observed that E2, after being rotated and having its major axis placed perpendicular to the tube axis, falls at a velocity that is 1/3 slower than that of the sphere and b) the solid S-S, the sphere is 2.47 times faster than E2.

Fig. 6. Photographs of solids of revolution: a) S-S, b) E2.

IV. DISCUSSION AND CONCLUSIONS

Following the principles of TPACK [10] and project didactic [8] it is considered that the traditional methods of teaching fluid mechanics have become insufficient to achieve the effective and significant learning required for undergraduate students. Various proposals [12,13] have been carried out prior to this work. The proposal of specific interdisciplinary projects, with advanced students from different backgrounds, can be a fruitful way to provide new thinking tools and skills. Creative thinking crosses the boundaries of a particular discipline. In this first phase, the contributions of the FADU intern student, co-

author of this work, encourage us to continue in this direction. Classical texts on teaching fluid mechanics usually only encompasses on the topic of Stokes' law in passing. It is often presented as solved problems to determine the terminal velocity of spheres [14], mentioned briefly at the end of topics such as drag on immersed bodies [15], in relation to the existence of blunt and streamlined contours [16], as flow over a sphere and cylinder: friction and pressure drag [17], as a method for measuring viscosity [18], as drag coefficients in common geometries [19], in the context of external flows [20], as experimental internal flows [21], and in relation to drag on spheres in laminar flow [22]. While some texts include the topic of creeping motion [23], it is necessary to refer to specific literature to address low Reynolds number flows [24], particularly when dealing with aspects such as the behaviour of non-spherical bodies.

One possible explanation for the brief theoretical treatment of low Reynolds number fluids in classical texts aimed at teaching fluid mechanics., is that flows with Re < 5 are exceptional in the classic applications of fluid mechanics in industrial engineering. But interests have changed and today the study of low to moderate Re flows is an interdisciplinary research field comprising also of various areas of engineering (electronics, industrial, environmental, food, petroleum, aeronautical), biology [25-26-27], physics, and robotics [28], among other academic disciplines. Recent works in computational fluid dynamics show the growing interest in studying the motion of non-spherical shapes at low Reynolds numbers [29-30-31-32-33].

It is considered that the experiences presented in this work are just an example of the many academic activities that allow for the integration of previous knowledge while providing new content and tools to undergraduate students. Experience III.A.1 and III.A.2 review error propagation, techniques for graphical representation of experimental data, simple statistical models, and introduces students to the problem of flow patterns at low to moderate Reynolds number. Experience III.A.3 discusses the predictive value of the differential equation for the motion of a falling sphere in a viscous flow, adimensionalization, and solving simple equations using their knowledge of numerical calculation. The study of deviation from sphericity is gradually introduced starting from river pearls (spheroids), to then, consider prolate shapes (ellipsoid model). The process of designing parts motivates the creativity of students in the conception of morphologies, or in the case of electronics-engineering students, in the introduction of improvements in electronic circuits, development of filters among other concerns.

From an experimental point of view, although there are simple commercial devices for measuring the viscosity of glycerine, such as the one proposed by Osaw Industrial Products PVT.LTD. [34], they do not allow for research projects involving objects that deviate from sphericity as proposed in this work. Experiments related to low Re numbers are usually referred to as simple experiences associated with

Stokes' law [35]. There are other devices proposed for teaching viscous fluid mechanics in universities, but with different objectives, such as several experiments for measuring the viscosity of aqueous glycerol solutions using a tank-tube viscometer [36]. These experiments are dedicated to chemical engineering students to introduce them to the concept of viscosity of a Newtonian fluid. The equipment presented in this paper is relatively simple to build, low cost, and versatile enough for carrying out multiple experiments.

It is considered that the presented experiments contribute to enrich the concept of viscosity and density, in terms of their role in establishing the type of regime (laminar or turbulent), the awareness of flow patterns according to the number of Re, the sensitivity of the drag force, not only to the fluid conditions, but also to the shape, size, surface, speed of the object the effect of walls at different distances on the flow behaviour [37], the concept of streamlining profile vs that of "bluff body" and the effect of textures or roughness on drag force [9]. Based on the teaching experiences carried out during the Covid-19 pandemic, virtual platforms for teaching fluids [38] have emerged, which not only allow students to access the theoretical foundations and measurements required during the practice, but also include images, animations, and explanatory videos demonstrating how the practice is conducted by teachers to support the theoretical content. Additionally, these platforms offer an immersive simulator as an additional tool for practicing the handling of the experimental installation, faithfully reproducing the operation of the practice. But, as of the date of this work, the topics covered on the platform are three practices/simulators: Head Loss in Pipes (FM-HLP), Flow in Open Channel (FM-OC), and Wind Tunnel (FM-WT)

Instruments are also being developed for the evaluation of learning in this type of experience. A future following up step, in addition to improving the equipment with the inclusion of more measurement modules, contemplates: a) experiences with circular disks and cylinders [39], b) the combination of shapes in 1, 2 or 3 dimensions, where the apparent surfaces and radii can be known and to study semi-empirical relationships (wetted surface vs. terminal velocity) [6], c) change the viscous fluid in the tube, d) the realization of scale models that reproduce natural forms of interest such as oblate spheroids [40] or platonic solids. It is considered that the described device provides an opportunity for students to carry out experiments for the acquisition of original experimental data, to apply their mathematical and computational skills, as well as statistical analysis to interpret experimental data with the aid of computer software. A future perspective does not rule out the possibility of creating a virtual laboratory activity that will be offered as a complement to the traditional syllabus in the labs for subsequent academic years. The teaching of fluid mechanics must adapt to the increasing importance that new technologies are having in higher education [41] and incorporate new tools that have emerged post-pandemic [42].

REFERENCES

[1] H. Brenner."Hydrodynamic Resistance of Particles at small Reynolds Numbers", *Advances in Chemical Engineering*, vol 6, pp. 287-438, 1966

[2] I. H. Shames. *Capítulo 7: "Análisis dimensional y semejanza"in La mecánica de los fluidos*, Madrid: McGraw Hill,1967, pp. 213-233

[3] S. F. Hoerner. Fluid-Dynamic Drag. Theoretical, experimental, and statistical information. Published by The autor. (1965).

[4] A. Vian and J, Ocón. Elementos de Ingeniería Química. Madrid. Aguilar. 1976. Tabla A2-14 P. 294-96.

[5] F.M White. Viscous Fluid Flow, New York. Mc Grow-Hill, pp243-246), 1974.

[6] W. Kunkel. "Magnitude and caracter of errors produced by shape factors in Stokes Law estimates of Particle radius". *J. Appl Phys*. 10, pp. 1056-1058, 1948.

[7] E. D. Antokoletz, H. Wziontek, C. N. Tocho, R. Falk. "Gravity reference at the Argentinean–German Geodetic Observatory (AGGO) by co-location of superconducting and absolute gravity measurements" Journal of Geodesy, pp. 94-81, 2000.

[8] R. Marbello Pérez. Manual de Prácticas de Laboratorio de Hidráulica", Escuela de Geociencias y Medio Ambiente, Universidad Nacional de Colombia, sede Medellín, Anexo A5: Propagación de errores, pp.315-318.

[9] Vogel, Life *in Moving Fluids: The Physical Biology of Flow*. 2.ed. Revised and Expanded, Princeton Univ. Press, 1996.

[10] J. M. Koehler, P. Mishra, and W. Cain. "What Is Technological Pedagogical Content Knowledge (TPACK)?", Volume 193, Number 3, 2013, Journal of Education, pp 13-19.

[11] C. Montellano Tolosa, C. Didáctica Proyectual. Santiago de Chile. Ediciones Universidad Tecnológica. 1 era. Ed. 1999.

[12] I. Ghersi, M. Miralles; El desarrollo del pensamiento creativo en estudiantes de ingeniería, ¿Formados para crear? Publicado en las memorias del Congreso Iberoamericano de Ciencia, Tecnología, Innovación y Educación, OEI, Buenos Aires, 12-14 de noviembre de 2014, ISBN 978-84-7666-210-6; Comunicación 651.; https://es.slideshare.net/crojas6/el-desarrollo-del-pesamiento-creativo-en-estudiantes-de-ingneireia-70192908ailen

[13] M. T. Miralles, A. A. Borches and A. I. Kessler, "Physical Thinking vs. Project Thinking: from Kaleidoscopes to Mutable Materials," *2021 Machine Learning-Driven Digital Technologies for Educational Innovation Workshop*, Monterrey, Mexico, 2021, pp. 1-4, doi: 10.1109/IEEECONF53024.2021.9733751.

[14] C. T. Crowe, D. F. Elger, J. A. Roberson. "Mecánica de Fluidos". Compañía Editorial Continental. 1era. Ed. México, 2002, pp. 492 – 497.

[15] V. L. Streeter. *Chapter 5*: "Viscous Efects in Fluid Resistance" in *Fluid Dynamics.* London McGraw Hill Book Company, 1962, p. 210.

[16] C. Mataix. *Capítulo 8. "*Resistencia de los fluidos en general" in *Mecánica de Fluidos y máquinas hidráulicas*. Madrid: Ediciones del Castillo, 2da. Ed., 1986, p. 199.

[17] R. W Fox, A. T. McDonald, P. J. Pritchard. *Chapter 9*: "External Incompressible viscous flow" in *Introduction to Fluid Mechanics*. John Willey &Sons. 6ta. Ed., 2004, pp. 438-440.

[18] B. Massey, Revised by J. Ward-Shmith. *Chapter 6:* "The measurement of visocosity" in *Mechanics of Fluids.*. Taylor &Francis, 6ta. Ed. 1989, pp. 210-220.

[19] Y, A, Cengel, J. M. Cimbala. *Capítulo 11*: "Flujo sobre cuerpos: arrastre y sustentación", in *Mecánica de Fluidos. Fundamentos y Aplicaciones*. Bogotá:Mc Grow Hill, 1era. Ed., 2006, pp. 571-574.

[20] M. C: Potter, D.C. Wiggert; T. I. P. Shih. *Capítulo 8*: "Flujos externos" in *Mecánica de Fluidos*. Thomson, 2005, pp. 306-307.

[21] F. M. White. *Chapter 7*: "Flow Past Immersed Bodies" in *Fluid Mechanics*. Milan: McGrow Hill, 8va. Ed., 2015, pp., 451-456.

[22] R. L. Mott. *Capítulo 17*: "Arrastre y sustentación" in *Mecánica de Fluidos*. 6ta. Edición. Pearson Educación. 2006, p.530.

[23] E. Krause. "Fluid Mechanics".Berlin: Springer- Verlag. 1965, p. 42.

[24] J. Happel, H. Brenner. "Low Reynolds number hydrodynamics with special applications to particulate media". Boston: Martinus Nishoff Publishers.1983.

[25] P. G. Brewer, E. T. Peltzer, K. Lage. "Life at low Reynolds Number Re-visited: The apparent activation energy of viscous flow in sea wáter". Deep -Sea Research Part I, 176,2021.

[26] B. U. Felderhof. "Stokesian swimming of a prolate spherid at low Reynolds number". *European Journal of Mechanics B/ Fluids*, 60, 2016, pp. 230-236.

[27] B. U. Felderhof. "Instantaneus swimming velocity of a body at low Reynolds number". *European Journal of Mechanics B/ Fluids*, 32, 2012, pp. 88-90.

[28] W. M. Nga, X. J. Tenga, Ch. Guob, C. Liub, S. Ch. Lowa, D. J. Chieh Chana, R. Mohamudc, J. Lima."Motion control of biohybrid microbots under low Reynolds number environment: Magnetotaxis", *Chemical Engineering & Processing: Process Intensification. 141,2019,107530.

[29] H. Sharma, B. S. More, G. Mourya, "Numerical analysis of triangular prism at low Reynolds number".*Materialstoday*: Proceedings 66, 3, 2022, pp. 1120-1125.

[30] P. Yu, R. Lu, W, He, L, K, B, Li. "Steady Flow around an inclined torus at low Reynolds numbers: Lift and drag coeffitiens". *Computers and Fluids*, 171, 2008, pp. 53-64.

[31] F. Dioguardi, D. Mele "A new shape dependent drag correlation formula for non-spherical rough particles. Experiments and results", *Powder Technology*. Volume 277, June 2015, pp. 222-230.

[32] K. O. Lund, D. Trees. "Low Reynolds -number momento on asymmetric bodies". *Experimental Thermal and Fluid Science*, 24, 2001, 61-66.

[33] R. Ouchene, M. Khalij. A. Taniere, B. Arecen. "Draf, lift and torque coeffcientes for elipsoidal particles: From low to moderate particle Reynolds numbers". *Computers & Fluids.*113, 2015, pp. 53-64.

[34] Instruction Manual for Vicosity of Glycerine(SK049). https://srisriuniversity.edu.in/wp-content/uploads/2017/09/Indosaw_VISCOSITY-SK049.pdf

[35] D. Leibovich, M. C. Molas, F. Rodrigez Riou. "Análisis de la velocidad de cuerpos esféricos en sustancias Viscosas"https://www.fisicarecreativa.com/informes/infor_termo/ley_stokes.pdf

[36] K. Kyung, P, Sammaiah, R. Sanjeev: "Experiments on viscosity oh aqeuous glycerol solutions using a Tank-Tube Viscometer*", Chemical Engineering Education*, summer 1999.

[37] C. M. White. "The drag of cylinders in fluids at low speeds" *Proc. Royal Soc. Lond*. A 186: pp. 472-79. 1946..

[38] P. L. A. Cruz del Álamo, P. Megía , J. Plaza , C. Casado, R. Van Grieken, F. Martínez, R. Molina, "FLUID-LABVIR, an immersive online platform as complement to enhance the student's learning experience in experimental laboratories of Fluid Mechanics and Fluid Engineering". *Education for Chemical Engineers* 41, October 2022, pp.1-13.

[39] Cox, P.L "The motion of long, slender bodies in a viscous fluid. Part 1, General Theory". J. *Fluid Mech*. vol 44, pp. 791-810, 1977.

[40] R. E. Zaret and W. Ch. Kerfoot. "The Shape and Swimming Technique of Bosmina Longirostris1: Swimming of Bosmina". *Limnology and Oceanography*, vol. 25, n.º1, pp. 126-33, 1980.

[41] R. Lamb. "Virtual reality and science, technology, engineering, and mathematics education" in *International Encyclopedia of Education (Fourth Edition)*, 2023, pp. 189-197.

[42] P. Dumka, R. Chauhan, A. Singh, G. Singh, D. Mishra."Implementation of Buckingham's Pi theorem using Python" in *Advances in Engineering Software*. Volume 173, November 2022.